

---

# TEXIM FAST: TEXT-TO-IMAGE REPRESENTATION FOR SEMANTIC SIMILARITY EVALUATION USING TRANSFORMERS

---

**Wazib Ansar**

A. K. Choudhury School of IT  
University of Calcutta  
Kolkata, West Bengal, India  
waakcs\_rs@caluniv.ac.in

**Saptarsi Goswami**

Department of Computer Science  
Bangabasi Morning College  
Kolkata, West Bengal, India  
sgakc@caluniv.ac.in

**Amlan Chakrabarti**

A. K. Choudhury School of IT  
University of Calcutta  
Kolkata, West Bengal, India  
acakcs@caluniv.ac.in

## ABSTRACT

One of the principal objectives of Natural Language Processing (NLP) is to generate meaningful representations from text. Improving the informativeness of the representations has led to a tremendous rise in the dimensionality and the memory footprint. It leads to a cascading effect amplifying the complexity of the downstream model by increasing its parameters. The available techniques cannot be applied to cross-modal applications such as text-to-image. To ameliorate these issues, a novel Text-to-Image methodology for generating fixed-length representations through a self-supervised Variational Auto-Encoder (VAE) for semantic evaluation applying transformers (TexIm FAST) has been proposed in this paper. The pictorial representations allow oblivious inference while retaining the linguistic intricacies, and are potent in cross-modal applications. TexIm FAST deals with variable-length sequences and generates fixed-length representations with over 75% reduced memory footprint. It enhances the efficiency of the models for downstream tasks by reducing its parameters. The efficacy of TexIm FAST has been extensively analyzed for the task of Semantic Textual Similarity (STS) upon the MSRPC, CNN/ Daily Mail, and XSum data-sets. The results demonstrate 6% improvement in accuracy compared to the baseline and showcase its exceptional ability to compare disparate length sequences such as a text with its summary.

**Keywords** Oblivious Inference · Sequence Embedding · Text-to-Image · Transformers NLP · Variational Auto-Encoder

## 1 Introduction

Text is a ubiquitous mode of communication, knowledge dissemination, and information preservation. It is the most convenient media to navigate and retrieve information concerning a topic from voluminous repositories [1]. The steady progress in the field of Natural Language Processing (NLP) has enabled seamless comprehension and generation of unstructured texts with high precision [2]. Considering the colossal amount of text at our disposal, research directed towards devising techniques for effective representation of unstructured textual content has become all the more essential [3]. Despite abundant research, most of them rely on generating multi-dimensional vector representations of text leading to the repercussions associated with the "curse of dimensionality" like huge memory footprint and exorbitant computational complexity of downstream tasks [4].

The text representation techniques are often domain-specific, i.e. the vector representation of a text sequence cannot be fed into an image-specific model. To bridge this gap between text and image, research must be directed towards formulating cross-modal approaches to generate image representations from text comprising the linguistic intricacies. A few studies have been conducted to replace text with equivalent images [5], or to produce modified illustrations [6–8]. But, none of these generate pictorial representations from textual embeddings that can equivalently be applied to both image and text-oriented models for downstream tasks.

Semantic Textual Similarity (STS) is one of the renowned tasks in NLP that revolves around assessing the level of semantic equivalence between pairs of sequences as a continuous value [9]. STS plays a pivotal role in NLP applications like Automatic Text Summarization (ATS) [10], Plagiarism Detection (PD) [11], Question Answering (QA) [12], and

Machine Translation (MT) [13]. STS goes beyond superficial similarity considering factors such as the overlap, order, and the length of common sub-sequences [14–16]. Rather it relies on ontology [17, 18], context [19], semantics [20, 21] accompanied with deep learning based architectures [22–25]. Although such approaches provide satisfactory results, they succumb while dealing with disparate sequence lengths such as comparing a text with its associated summary.

To address the research gaps stated above, we direct our research towards devising an innovative "Text-to-Image" (TexIm) encoding. These cross-modal encodings are memory-efficient, can be visualized as an image, and assimilate the linguistic intricacies of the input text. This paper is an improvement over the contribution by Ansar et al. [26] whereby they generated informed pictorial representations of texts capturing the contextualized syntactic and lexical features using BERT with 37.37% reduced memory footprint. However, this approach had some drawbacks, namely- (1) the size of the representations varied according to sequence lengths as it assigned each word as a pixel requiring padding to ensure uniform lengths, (2) this reduced its effectiveness while comparing representations of disparate sequence lengths, (3) the Principal Component Analysis (PCA) applied for dimension reduction led to loss of information. To mitigate these shortcomings, we hereby put forth our endeavor coined as **TexIm FAST** for Text-to-Image conversion with Fixed-length representations applying Autoencoder for Semantic evaluation through Transformers. It includes a novel Variational Auto-Encoder (VAE) based on Convolutional Neural Network (CNN) and Transformer with Selective Learn-Forget Network (TSLFN) to encode the input text into fixed-length pictorial representations occupying less than 75% memory. Furthermore, a weighted annealing mechanism is applied to the VAE to ameliorate posterior collapse wherein the latent variable becomes uninformative and gets ignored by the decoder [27]. Compared to the previous TexIm rendition- (1) It encodes the entire sequence as a whole instead of word-level representations. (2) It eliminates the bias infused due to variable-length sequences. (3) It generates the pixels using a self-supervised VAE eliminating the need for any annotated data-sets. Besides, it allows oblivious inference through encoded pictorial representations that can be utilized for further analysis without revealing the actual text [28]. As a downstream task, a novel architecture utilizing TSLFN has been proposed for STS. Its performance on STS demonstrates its exceptional ability to deal with disparate-length sequences. The principal contributions of this paper are as follows:

1. We propose TexIm FAST, an improved Text-to-Image encoding technique that allows oblivious inference retaining the semantic information in the text with over 75% reduction in memory footprint.
2. It comprises a self-supervised CNN-TSLFN based VAE to capture the contextualized semantic information in a sequence holistically and encode it into a uniform-dimensional image irrespective of its length.
3. The efficacy of the pictorial representations can be observed through 5.6% higher accuracy over the baseline for STS task applying a novel TSLFN architecture.

The remainder of this paper has been outlined herein. *Section 2* presents the literature surveyed. *Section 3* enunciates the methodology of the proposed TexIm FAST. *Section 4* provides the details of the experiment conducted. *Section 5* showcases the results obtained through extensive evaluation. Finally, the conclusions are drawn and the future scope is discussed in *Section 6*.

## 2 Related Works

In this section, a review of the preceding works has been undertaken to assess the inherent gaps in research. For ease of comprehension, the commentary of works has been grouped under subsections dedicated to cross-modal representations and semantic similarity.

### 2.1 Cross-Modal Representation

The related works can be segregated into cross-modal matching as-well-as generation of cross-modal representations. For cross-modal matching, Yang et al. [29] developed a quantization algorithm with shared predictive-representations and label alignment. Xu et al. [30] proposed cross-modal matching with co-attention-based alignment of image regions with words in textual descriptions along with global semantic prediction of labels. Jin et al. [31] devised a CNN-based cross-modal matching model with a specialized hashing technique exploiting spatial information to target efficiency.

A few notable works on cross-modal generation have been discussed herein. Zakraoui et al. [5] substituted text with the most probable illustrations from a repository. Das et al. [32] applied stack Generative Adversarial Network (GAN) and Long Short-Term Memory (LSTM)-based autoencoders. Ramesh et al. [33] formulated a zero-shot learning-based transformer. Saharia et al. [34] utilized pre-trained language models for encoding text accompanied by a diffusion model for image generation. Gu et al. [35] constructed a VAE with a quantized vector in association with a diffusion model. Tan et al. [36] generated images from textual captions applying GAN with spatial attention and VAE for normalized

latent distributions. In these works, the generated illustrations are devoid of the linguistic characteristics of the original text. This limits their application to downstream NLP tasks.

Besides, a handful of research has been conducted to generate visual representations of text capturing its linguistic intricacies. Nataraj et al. [6] converted text into grayscale images having pixels with varying intensity values corresponding to the characters. The images were reported to be immune to API injection and obfuscation of code for the application of malware detection. He et al. [7] further improved it through Spatial Pyramid Pooling (SPP) to accommodate inputs having variable lengths. Petrie et al. [8] focused on string-map visualizations for patent-inventor record comparison. From the above-mentioned contributions, it can be inferred that textual content can be transformed into cross-modal representations flexible enough to be processed either as text or as images.

## 2.2 Semantic Similarity

The primeval works on evaluating the similarity between texts focused on identifying common sub-sequences. A few such similarity measures are even prevalent in the efficacy evaluation of summarization or translation models in NLP. Chin-Yew Lin [14] proposed a recall-oriented metric relying on the overlap of n-grams to determine the similarity among a pair of texts. Contrastingly, Papineni et al. [15] computed the similarity through a precision-oriented metric with a penalty term to account for disparate sequence lengths. However, these approaches relied on superficial factors including overlap, order, and common sub-sequence length [16].

Besides identifying common sub-sequences, STS takes into account ontology, context as-well-as semantics of sequences. Sánchez and Batet [17] calculated through the context of terms inferred from the ontological knowledge base. To mitigate the restriction imposed by predefined ontologies, Jiang et al. [18] formulated a feature-oriented approach utilizing Wikipedia as the knowledge base. The Cilibrasi and Vitanyi [19] calculated the similarity of words by constructing the context depending on Google search results. Kusner et al. [20] calculated semantic similarity as the minimum distance between the embeddings of a word in one sequence and its nearest word in the other sequence. Wang et al. [21] decomposed the sentences for comparison into words and calculated the cosine similarity among them. The recent trend reflects the inclination towards deep learning models. He and Lin [22] combined Bi-LSTM with CNN for modeling the context followed by a pair-wise comparison of the hidden states. Tien et al. [23] proposed an LSTM-based similarity prediction architecture utilizing sentence embeddings constructed by a CNN-LSTM architecture. Lopez-Gazpio et al. [24] formulated an attention-based model taking n-grams as inputs to construct attention vectors for the sentence pairs and fed them to an aggregation layer. Li et al. [25] proposed a cross-self attention-based Siamese Neural Network for determining the semantic similarity of biomedical texts. A common drawback of STS approaches is that they falter with disparate-length sequences.

These developments show that cross-modal representations expand the horizons for processing data. Besides, techniques like quantization, hashing, or latent representation generation facilitate memory-efficiency. Moreover, semantic similarity is one of the prominent tasks in NLP to assess the efficacy of textual representations. However, devising a light-weight model capable enough to capture the linguistic intricacies of cross-modal representations with disparate length sequences effectively is a challenging task.

## 3 Proposed Methodology

The proposed methodology has been segregated into two coherent sub-sections- *Section 3.1* describes the proposed TexIm FAST for the generation of pictorial representations from the text. While *Section 3.2* presents the novel TSLFN-based architecture for evaluation of the TexIm FAST representations upon the downstream task of STS.

### 3.1 TexIm FAST

The flow steps in the proposed TexIm FAST have been elucidated herein-below:

#### 3.1.1 Pre-processing

The input text is first put through cleaning processes to remove irrelevant portions like line breaks, tabulations, URL patterns, numbers, non-ASCII characters and punctuations. Standardization of white space is performed.

#### 3.1.2 Tokenization

The pre-processed text undergoes sub-word tokenization wherein a word is split into meaning preserving morphemes [37]. This reduces the vocabulary size by allowing different words to be formed through the combination of a given set

---

**Algorithm 1** Tokenization Lookup Table Generation

---

**Require:** Vocabulary  $V$

**Ensure:** Tokenization Lookup  $T_{id}$

```

 $l_V \leftarrow |V|$   $\triangleright l_V$  is the size of  $V$ 
for  $i \leftarrow 0$  to  $(l_V - 1)$  do
     $T_{id}[i] \leftarrow \{V_i : t[i]\}$   $\triangleright V_i$  is mapped to  $t[i]$ 
end for

```

---

of sub-words. For instance, words like "walk", "walking", "talk" and "talking" can be tokenized into ["walk", "talk" and "##ing"]. Moreover, it improves comprehension by rendering meaning to its constituent sub-words. For instance, from the tokens like "snow", "man", and "fire", words like "snow", "snowman", "fire" and "fireman" can be formed. A lookup table is constructed wherein each sub-word in the vocabulary  $V$  is assigned a unique integer identifier  $t[i]$  ranging from 1 to  $|V|$  as portrayed in Algorithm 1. Relying on it, a tokenized sequence of integers  $S_t$  is obtained such that  $V_i$  in the sequence is replaced with its corresponding integer identifier  $t_{id}[i]$ . To ensure uniform sequence length  $L$ , padding token(s) are appended as depicted in equation (1).

$$S_t[i] = \begin{cases} t_{id}[i] & \text{for sub-word tokens} \\ 0 & \text{for padding} \end{cases}, \forall i \in [0, sl) \quad (1)$$

### 3.1.3 Input Embedding

The text is then transformed to a sequence of embeddings  $S_e$  such that each token  $S_t[i]$  in the sequence is replaced with a unique vector  $e[i]$ . The embeddings are randomly initialized as  $d$  dimensional vectors and optimized during training just as other network parameters. For contextualized representation, position embedding is applied to the sequence to establish the ordering of the tokens. For this, the positional index  $S_p[i]$  of the  $i^{th}$  token in the sequence is determined using equation (2).

$$S_p[i] = \begin{cases} \theta + i\delta & \text{for sub-word tokens} \\ -1 & \text{for padding} \end{cases}, \forall i \in [0, sl) \quad (2)$$

where  $\delta$  is the increment value with  $\theta$  serving as the offset. The  $d$  dimensional position embeddings are then learnt during network training utilizing  $S_p$ . Finally, the tokenized integer sequence  $S_t$  and the position encoded sequence  $S_p$  are element-wise concatenated (denoted by  $\oplus$ ) to obtain the embedded sequence  $S \in \mathbb{R}^{L \times D}$  as shown in equation (3).

$$S = S_p \oplus S_t \quad (3)$$

### 3.1.4 Low-Dimensional Projection

The embedded input sequence is transformed to a low-dimensional fixed-length vector from which the TexIm FAST encodings can be derived. To accomplish this, a novel VAE architecture based on CNN and TSLFN has been formulated as depicted in Figure 1. The model is trained through a self-supervised learning mechanism wherein it takes reference for the output from the input itself [38]. A merit of the proposed VAE is that it encodes any variable-length sequence into a fixed-length representation. This helps to generate images of equal resolution irrespective of their input sequence lengths. The salient features of the model have been presented as follows:

- (i) **Transformer with SLFN (TSLFN):** It comprises of Multi-Head Attention (MHA) followed by a Selective Learn-Forget Network (SLFN) as depicted in Figure 2. The MHA  $Att^m$  concatenates  $H$  self-attention units  $Att^s$  projected through  $W^o \in \mathbb{R}^D \times \mathbb{R}^D$  to accommodate parallel computation involving diverse positions [39] as expressed in equations (4) and (5).

$$Att^s = softmax\left(\frac{Q_s K_s^T}{\sqrt{D}}\right) V_s \quad (4)$$

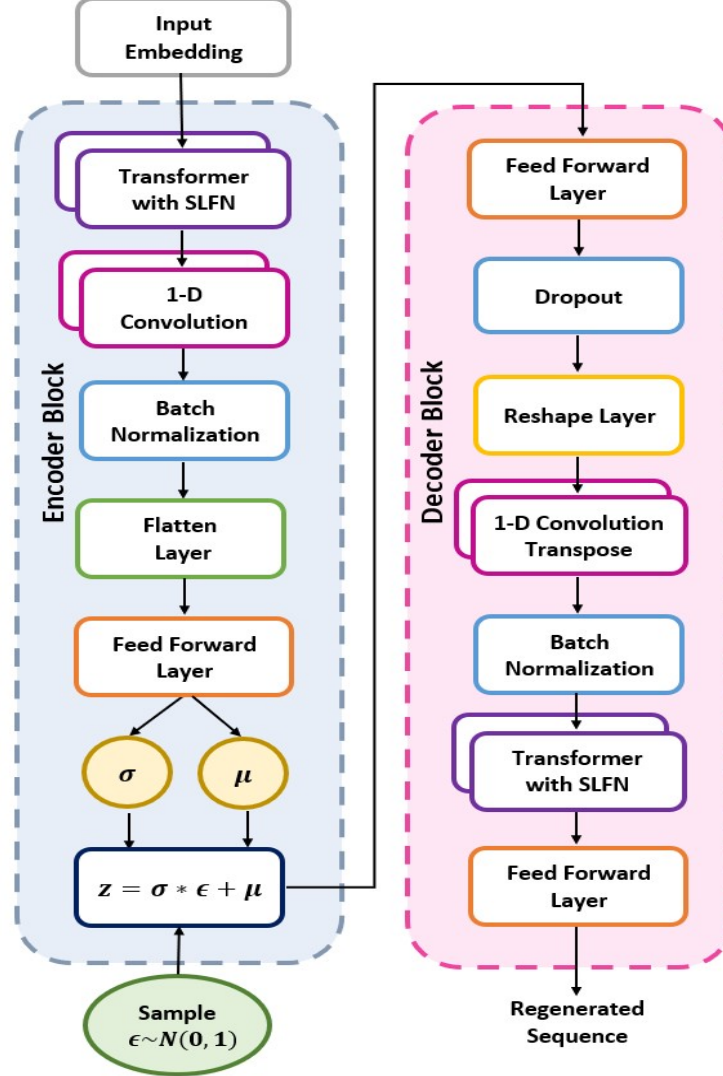


Figure 1: Illustration of the proposed TexIm FAST VAE architecture for projection of sequences to fixed-length vector

$$Att^m = Concatenate(Att_i^s)W^o, \forall i \in H \quad (5)$$

where, query  $Q_s$ , key  $K_s$  and value  $V_s$  are calculated through linear transformations on the sequence  $Z \in \mathbb{R}^L \times \mathbb{R}^D$  along with weight matrices  $W^q$ ,  $W^k$  and  $W^v \in \mathbb{R}^{D \times \frac{D}{H}}$  as formulated in equation (6).

$$Q_s, K_s, V_s = W^q Z, W^k Z, W^v Z \quad (6)$$

The SLFN [40] augments the efficacy of the residual connections by effectively capturing the dependencies. It filters insignificant information reducing the overall complexity. It achieves selective learning through a gated mechanism involving a combination of sigmoid  $Sg_i$  and tanh  $Tg_i$  gates to update the hidden state  $H_i$  as shown in equation (7).

$$H_i = Sg_i + (Sg_i \odot Tg_i) \quad (7)$$

given that,

$$Sg_i = \sigma[(X_i W_i^s) + (H_{i-1} U_i^s)] \quad (8)$$

$$Tg_i = \tanh[(X_i W_i^t) + (H_{i-1} W_i^t)] \quad (9)$$

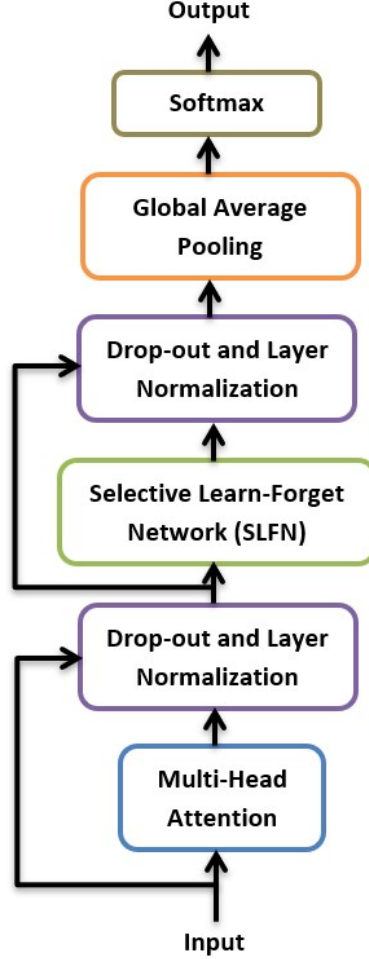


Figure 2: Illustration of the TSLFN architecture [40]

where,  $X_i$ ,  $H_{i-1}$ ,  $W_i^s$  and  $U_i^s$  denote the  $i^{th}$  step input, previous step hidden state, input weight matrix and the hidden state weight matrix respectively.

- (ii) **1-D Convolution:** It applies multiple linear filters over a sequence in a feed-forward fashion to extract meaningful features through sparse interactions and parameter sharing [41]. Given a sequence  $X \in \mathbb{R}^{L \times D}$ , a filter  $F_c \in \mathbb{R}^{F \times D}$  performs successive element-wise products over subsets  $S_f \in \mathbb{R}^{F \times D}$ ;  $\forall S_f \in X$  to generate a feature map  $F_m \in \mathbb{R}^{(L-F+1) \times D}$  as portrayed in equation (10).

$$F_m[i] = F_c \odot X_{i:i+F-1}, \forall i \in [0, (L - F)] \quad (10)$$

where  $X_{i:j}$  denotes a sub-set of  $X$  from position  $i$  to  $j$ .

- (iii) **Reparameterization and Objective Function:** Utilizing the mean  $\mu$  and standard deviation  $\sigma$  produced by the encoder, a Gaussian distribution is generated. A latent vector  $z$  is sampled from it as shown in equation (11).

$$z \sim \mathcal{N}(\mu, \sigma) \quad (11)$$

To make the sampling process continuous and differentiable, reparameterization is performed sampling  $\epsilon$  from a standard Gaussian distribution, i.e.  $\epsilon \sim \mathcal{N}(0, 1)$  and recomputing  $z$  as follows [42]:

$$z = \sigma * \epsilon + \mu \quad (12)$$

For training the network, Evidence Lower Bound (ELBo)  $J_{\text{VAE}}(\theta, \phi; x)$  [42] has been considered the objective function. It consists of the reconstruction loss  $\mathbb{E}_{z \sim q(z|x; \phi)} [\log p(x|z; \theta)]$  and the Kullback-Leibler (KL) divergence  $D_{\text{KL}}()$  between the encoded distribution  $q(z|x; \phi)$  and the required prior distribution  $p(z)$  as shown in equation (13) with  $x, \phi$  and  $\theta$  denoting the input, the encoder and the decoder parameters respectively.

$$J_{\text{VAE}}(\theta, \phi; x) = D_{\text{KL}}(q(z|x; \phi) || p(z)) - \mathbb{E}_{z \sim q(z|x; \phi)} [\log p(x|z; \theta)] \quad (13)$$

To avoid posterior collapse, a varying weight term  $W_a$  increasing with the training epochs is multiplied to  $D_{\text{KL}}(q(z|x; \phi) || p(z))$  as follows:

$$W_a = (1 + e^{-(\frac{n}{N} + b)})^{-1} \quad (14)$$

where,  $n, N, b \in \mathbb{N}$  denote the current epoch, total number of epochs and the control parameter. This is analogous to the annealing process and lays more emphasis on reconstruction loss. The modified ELBo  $J'_{\text{VAE}}(\theta, \phi; x)$  has been portrayed in equation (15).

$$J'_{\text{VAE}}(\theta, \phi; x) = W_a * D_{\text{KL}}(q(z|x; \phi) || p(z)) - \mathbb{E}_{z \sim q(z|x; \phi)} [\log p(x|z; \theta)] \quad (15)$$

### 3.1.5 Normalization and Feature Scaling

The fixed-length sequence embedding  $E$  having  $dim_e$  dimensions obtained in the preceding step requires additional processing to be considered as pixel intensity values. The components are normalized within the range of [0, 1] to achieve this (equation (16)). These normalized embeddings  $E'$  are then scaled between acceptable grayscale image intensity ranges, i.e. [0, 255] and  $E^s$  is obtained as shown in equation (17).

$$E' = \frac{e_i - \min(E)}{\max(E) - \min(E)}, \forall e_i \in E \quad (16)$$

$$E^s = e'_i * 255, \forall e'_i \in E' \quad (17)$$

---

#### Algorithm 2 Reshaping the Embedding Sequence

---

**Require:** Scaled Embedding Sequence  $E^s$  of length  $dim_e$

**Ensure:**  $I_l \times I_b$  dimensional Embedding Matrix  $E^G$

$E^G \leftarrow I_l \times I_b$  dimensional matrix initialized with zeros

$k \leftarrow 0$

**for**  $i \leftarrow 0$  to  $(I_l - 1)$  **do**

**for**  $j \leftarrow 0$  to  $(I_b - 1)$  **do**

$E^G[i, j] \leftarrow uint8(E^s[k])$

        ▷ Converting to 'uint8'

$k \leftarrow k + 1$

**end for**

**end for**

---

### 3.1.6 Reshaping and Quantization

A typical image has two dimensions as opposed to the one-dimensional normalized and scaled sequence that was created in the previous phase. Reshaping process is used to change this one-dimensional sequence into a two-dimensional shape as portrayed in Algorithm 2. The dimensions of the image matrix are predefined subject to the following constraint:

$$I_l \times I_b = dim_e \tag{18}$$

where,  $I_l$  denotes the image length,  $I_b$  the image breadth and  $dim_e$  the embedding dimension as-well-as the length of the scaled sequence. This guarantees that all images have the same dimensions. Finally, this matrix is utilized to generate the grayscale image. Here, the pixels are converted into an 8-bit unsigned int (or 'uint8') notation. Compared to the standard 32-bit floating point ('float32') notation, this aids in reducing the memory footprint. The generated image representations can now be applied to downstream NLP tasks.

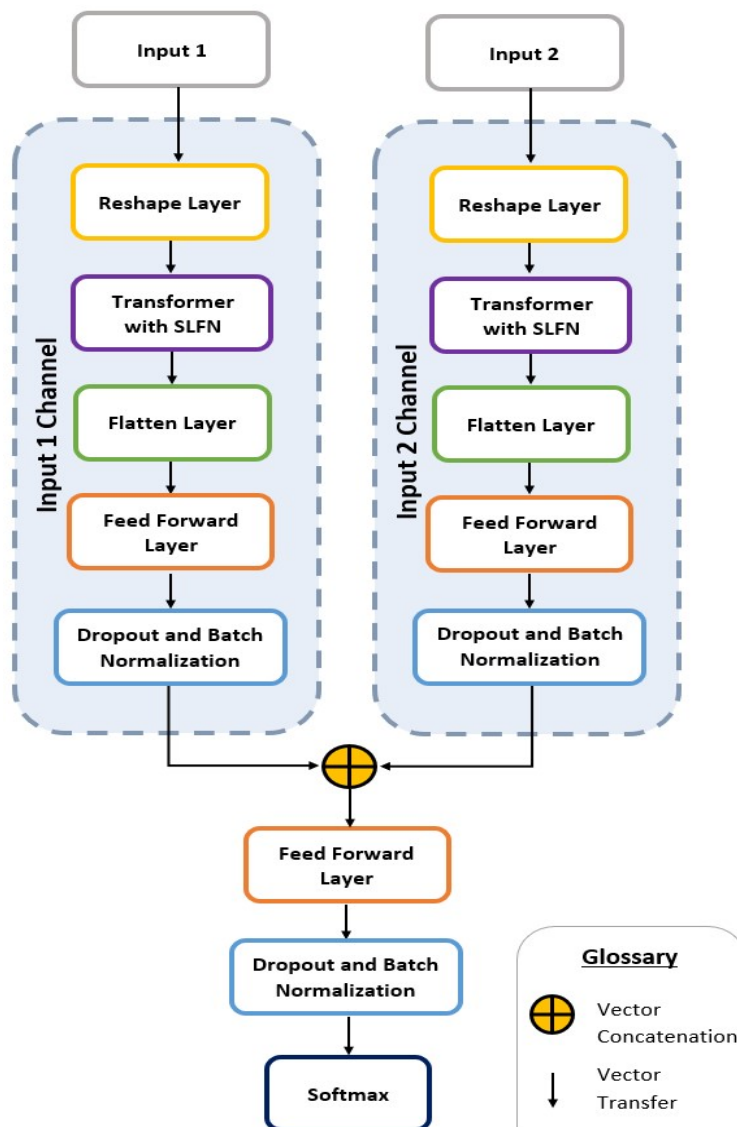


Figure 3: Illustration of the proposed TSLFN-based STS model



### 3.2 Architecture for STS Determination

To evaluate the efficacy of the TexIm FAST representations, a downstream STS task has been designed. For this, a novel transformer-based architecture has been devised for cross-modal determination of STS as illustrated in Figure 3. The architecture accepts two TexIm FAST images for comparison and outputs the similarity among them analogous to prevalent deep learning-based STS models in NLP [22, 25]. The inputs are propagated through two separate channels to obtain the hidden representations. Each channel includes a TSLFN block having architecture as shown in Figure 2. The hidden representations are then concatenated and processed further in the subsequent layers to predict their similarity. The proposed STS architecture is potent enough to analyze lengthy sequences despite being light-weight with less parameters.

## 4 Experiment Details

In this section, the experiment details such as the data-sets involved, implementation details as-well-as hyperparameter details of the proposed methodology have been enunciated.

### 4.1 Data-Sets

- **Microsoft Research Paraphrase Corpus (MSRPC):** It is a STS data-set released by Dolan and Brockett [43]. It comprises 5,801 pairs of sentences derived from news articles covering a range of topics. Each pair of sentences has been annotated as either similar or dissimilar in the form of a binary label. Out of the total pair of sentences, 3,900 pairs are paraphrases with the rest being dissimilar. The average length of the sentences is 18.92 words.
- **CNN/ Daily Mail:** It is an ATIS data-set put forth by Nallapati et al. [44]. It comprises news articles with their summaries (highlights) retrieved from the CNN<sup>1</sup> and the Daily Mail websites<sup>2</sup>. For implementation on STS task, for 143,408 samples out of 286,817 sequences, the summaries have been shuffled. While for the rest, the summaries correspond to the original news. Additionally, a column has been added to denote whether the text and the summary are similar or not. For the news sequences, the overall length is 766 words distributed among 29.74 sentences. Whereas the highlights approximately contain 53 words over a span of 3.72 sentences.
- **XSum:** It has been curated by Narayan et al. [45] from BBC News<sup>3</sup> for ATIS. The data-set comprises articles along with the headlines as its summary. This data-set has been modified for STS such that 102,022 sequences have summaries corresponding to the given news and 102,023 sequences have the summaries shuffled. It consists of an additional column to indicate the similarity between the news article and its summary. Overall, the articles are 431.07 words spanning 19.77 sentences. Besides, the headlines consist of 23.26 words and are single sentences.

### 4.2 Implementation Details

The methodologies proposed in this paper have been implemented on a Python 3 Compute Engine with Nvidia T4 GPU, 32 GB RAM, and 108 GB Disk in Google Colab<sup>4</sup>. The maximum sequence lengths of the inputs corresponding to the MSRPC, CNN/ Daily Mail, and XSum data-sets are 64, 768, and 512 respectively. The output representations are grayscale images of size  $(32 \times 16) = 512$  pixels.

### 4.3 Hyperparameter Details

The hyperparameters of both the TexIm FAST model and the STS model have been finalized through Random Search based hyperparameter optimization. The final set of hyperparameters for the TexIm FAST and the STS model has been presented in Table 1 and Table 2 respectively.

## 5 Results and Discussion

In this section, an extensive analysis of the results obtained from implementation of the proposed TexIm FAST has been performed on a variety of parameters and metrics.

<sup>1</sup><https://www.cnn.com>

<sup>2</sup><https://www.dailymail.co.uk>

<sup>3</sup><https://www.bbc.com/>

<sup>4</sup><https://colab.research.google.com>

Table 1: Hyperparameter Details of TexIm FAST

Hyperparameter	Value
#Transformer Blocks	2
# Attention Heads	4
#Convolutional Blocks	2
Activation Function	GELU
Dropout Ratio	0.3
Optimizer	Adam
Learning Rate	0.01
Train-Validation Split Ratio	80:20
Early Stopping Patience Value	2
Batch Size	16
Training Epochs	15

Note- GELU: Gaussian Error Linear Unit

Table 2: Hyperparameter Details of the STS Model

Hyperparameter	Value
# Transformer Blocks	1
# Attention Heads	4
Activation Function	LeakyReLU
Dropout Ratio	0.3
Optimizer	Adam
Loss Function	Binary Cross-Entropy
Learning Rate	0.01
Train-Validation-Test Split Ratio	70:15:15
Early Stopping Patience Value	5
Batch Size	16
Training Epochs	50

Note- Leaky RELU: Leaky Rectified Linear Unit

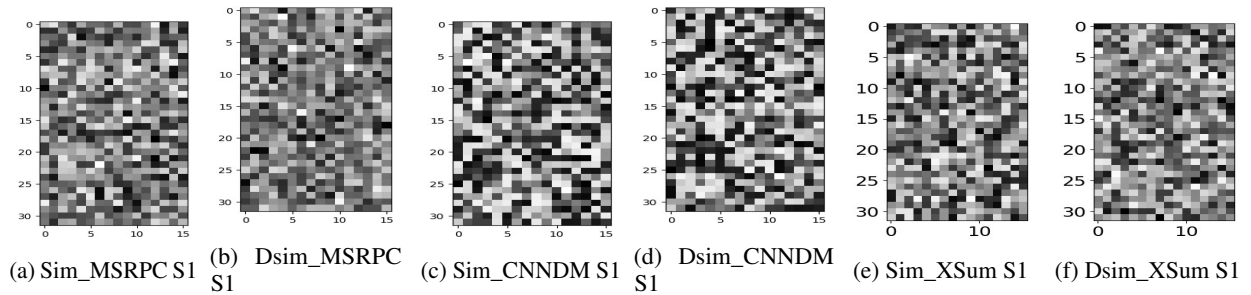


Figure 5: TexIm FAST representations corresponding to the first sequences for all the comparison objectives

Table 3: Demonstration of TexIm FAST

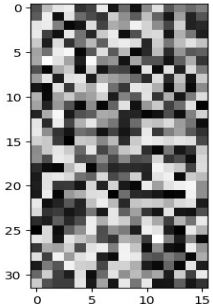
<p><b>Text:</b>  <i>Ever noticed how plane seats appear to be getting smaller and smaller? With increasing numbers of people taking to the skies, some experts are questioning if having such packed out planes is putting passengers at risk. They say that the shrinking space on aeroplanes is not only uncomfortable- it's putting our health and safety in danger. More than squabbling over the arm rest, shrinking space on planes putting our health and safety in danger? This week, a U.S consumer advisory group set up by the Department of Transportation said at a public hearing that while the government is happy to set standards for animals flying on planes, it doesn't stipulate a minimum amount of space for humans. 'In a world where animals have more rights to space and food than humans,' said Charlie Leocha, consumer representative on the committee. 'It is time that the DOT and FAA take a stand for humane treatment of passengers.' But could crowding on planes lead to more serious issues than fighting for space in the overhead lockers, crashing elbows and seat back kicking? Tests conducted by the FAA use planes with a 31 inch pitch, a standard which on some airlines has decreased . Many economy seats on United Airlines have 30 inches of room, while some airlines offer as little as 28 inches. Cynthia Corberrt, a human factors researcher with the Federal Aviation Administration, that it conducts tests on how quickly passengers can leave a plane. But these tests are conducted using planes with 31 inches between each row of seats, a standard which on some airlines has decreased, reported the Detroit News. The distance between two seats from one point on a seat to the same point on the seat behind it is known as the pitch. While most airlines stick to a pitch of 31 inches or above, some fall below this. While United Airlines has 30 inches of space, Gulf Air economy seats have between 29 and 32 inches, Air Asia offers 29 inches and Spirit Airlines offers just 28 inches. British Airways has a seat pitch of 31 inches, while easyJet has 29 inches, Thomson's short haul seat pitch is 28 inches, and Virgin Atlantic's is 30-31. Experts question if packed out planes are putting passengers at risk. U.S consumer advisory group says minimum space must be stipulated.</i></p>	
---	---

Figure 4: TexIm FAST representation

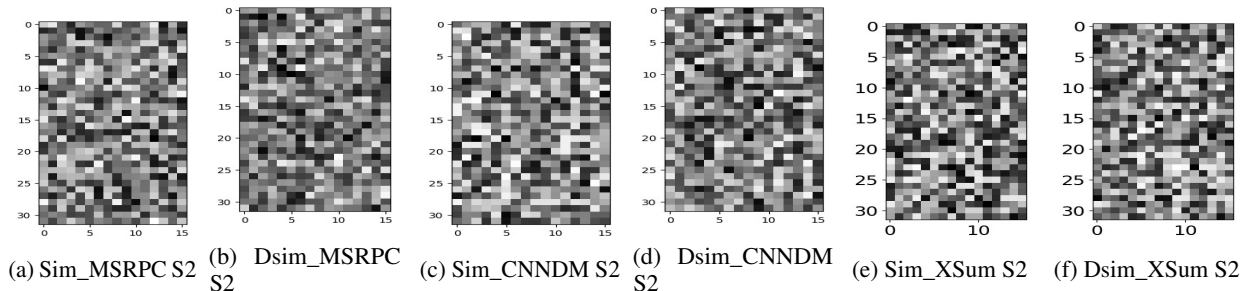


Figure 6: TexIm FAST representations corresponding to the second sequences for all the comparison objectives

### 5.1 Demonstration of TexIm FAST

The text and the associated graphic representation created by TexIm FAST are shown in Table 3 and Figure 4, respectively, as part of the suggested methodology’s demonstration. Each pixel in the visual representation represents a component of the low-dimensional sentence vector and expresses its value as pixel intensity. The pixels might not appear revealing enough at first glance. However, it incorporates the contextualized linguistic information from the text such that if two pictorial representations resemble one another, their provided texts must be semantically similar.

### 5.2 Comparison of Pictorial Representations

To validate the capability of the pictorial representations generated by TexIm FAST in retaining the information in text, the following comparison objectives have been formulated:

- (i) **Comparing Similiar Texts:** The TexIm FAST representations corresponding to the pairs of semantically equivalent texts from MSRPC, CNN DailyMail, and XSum data sets have been compared giving rise to objectives *Sim\_MSRPC*, *Sim\_CNNDM* and *Sim\_XSum* respectively. In *Sim\_MSRPC*, the compared texts have similar lengths. Whereas in *Sim\_CNNDM* and *Sim\_XSum*, disparate length sequences involving a text and its summary have been analyzed.

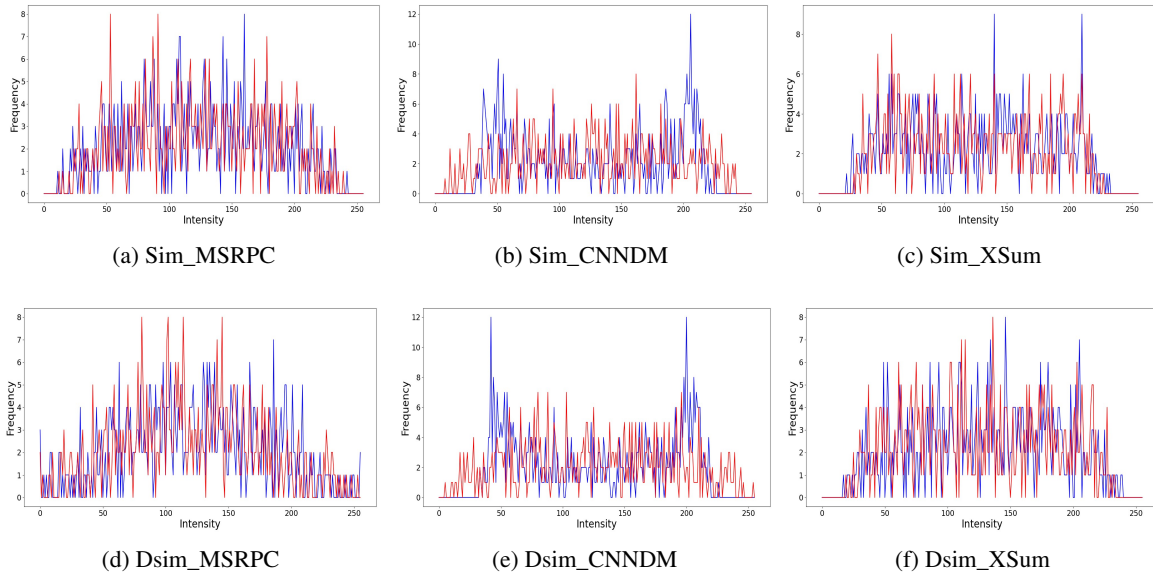


Figure 7: Comparison of the histograms of the TexIm FAST representations for all the comparison objectives

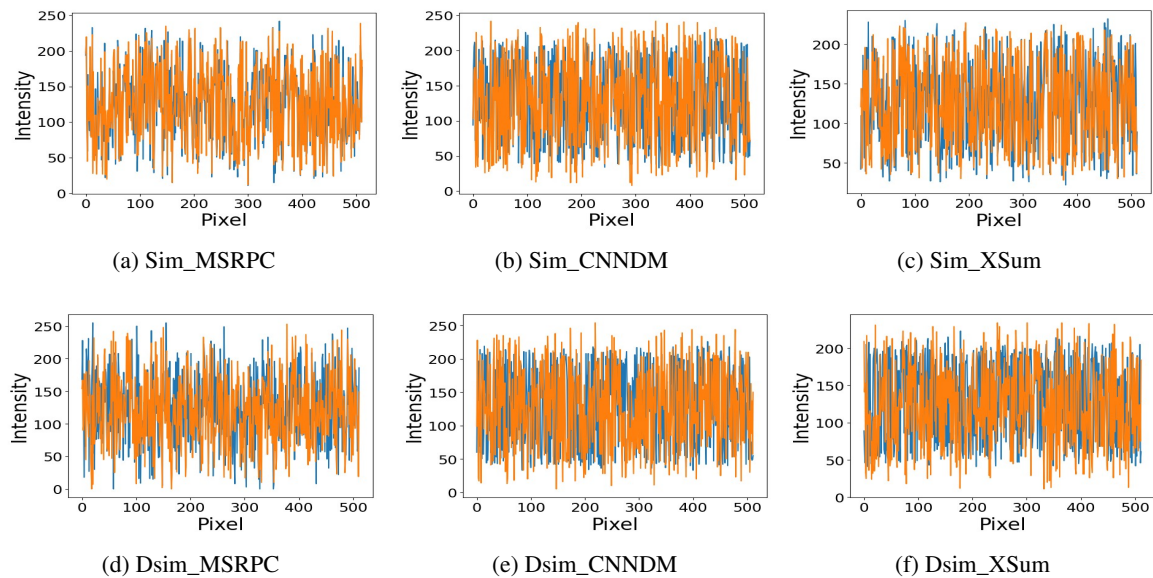


Figure 8: Comparison of the line plots of the TexIm FAST representations for all the comparison objectives

- (ii) **Comparing Dissimilar Texts:** The TexIm FAST representations of two semantically dissimilar texts have been compared to form the objectives  $Dsim\_MSRPC$ ,  $Dsim\_CNNDM$  and  $Dsim\_XSum$  corresponding to MSRPC, CNN DailyMail, and XSum data sets respectively. In  $Dsim\_MSRPC$  two semantically dissimilar texts having similar lengths have been considered. While in  $Dsim\_CNNDM$  and  $Dsim\_XSum$ , a text and the summary of some other dissimilar text with considerably smaller length have been examined.

Figure 5 and Figure 6 present the TexIm FAST representations of sequences for all the comparison objectives. Whereas, Figure 7 illustrates the comparison of the histograms. Since a histogram only reflects the frequencies of individual intensities, Figure 8 plots the pairwise pixel values for a better comparison between individual pixels. The results indicate that TexIm FAST captures the contextualized semantic information in the text and is potent enough to distinguish between similar and dissimilar texts. Furthermore, it is robust against the bias due to disparate sequence lengths as it effectively comprehends the (dis)similarity between long texts and concise summaries. This can be attributed to the ability to construct fixed-length representations from varying-length sequences.

Table 4: Comparison of Performance

Data-Set	Method	Accuracy	F1-Score
MSRPC	BLEU [15]	0.58	0.60
	ROUGE [14]	0.69	0.67
	WMD [20]	0.57	0.58
	S2SA-SNN [25]	0.67	0.62
	TexIm V1 [26]	0.68	0.66
	TexIm FAST-C	0.70	0.61
	<b>TexIm FAST</b>	<b>0.71</b>	<b>0.63</b>
CNN/ DailyMail	BLEU [15]	0.50	0.33
	ROUGE [14]	0.50	0.34
	WMD [20]	0.70	0.70
	S2SA-SNN [25]	0.52	0.52
	TexIm V1 [26]	0.63	0.60
	TexIm FAST-C	0.73	0.70
	<b>TexIm FAST</b>	<b>0.81</b>	<b>0.80</b>
XSum	BLEU [15]	0.50	0.33
	ROUGE [14]	0.52	0.35
	WMD [20]	0.69	0.68
	S2SA-SNN [25]	0.50	0.50
	TexIm V1 [26]	0.60	0.57
	TexIm FAST-C	0.72	0.70
	<b>TexIm FAST</b>	<b>0.80</b>	<b>0.79</b>

### 5.3 Performance Evaluation

The performance of the proposed TexIm FAST representations has been evaluated for the task of STS through comparison with the following works:

- (i) **ROUGE**: Recall-Oriented Understudy for Gisting Evaluation (ROUGE) metric proposed by Chin-Yew Lin [14] which relies upon the overlap of sub-sequences or n-grams to determining the similarity among a pair of texts.
- (ii) **BLEU**: Bilingual Evaluation Understudy (BLEU) metric proposed by Papineni et al. [15] to compute the similarity among two pieces of text. Unlike ROUGE, it is a precision-oriented metric with a penalty term to account for disparate sequence lengths.
- (iii) **WMD**: Word Mover Distance (WMD) by Kusner et al. [20] is a metric to ascertain the minimum distance for transportation of word embeddings from one document to the other.
- (iv) **S2SA-SNN**: A Siamese Neural Network based on BiLSTM with cross-self attention proposed by Li et al. [25] for determining the semantic similarity.
- (v) **TexIm V1**: Text-to-Image (TexIm) encoding technique for generating informed as-well-as memory efficient visual representation of text utilizing BERT-based contextualized embeddings [26]. These encodings are then fed into the proposed STS model.
- (vi) **TexIm FAST-C**: A variation of the proposed TexIm FAST devoid of the TSLFN block in the VAE, i.e. comprising only the convolutional blocks.

From the comparison with related works in Table 4, it can be observed that the BLEU and ROUGE falter in the case of long sequences as they are suited for short sequences. A contrasting observation is noted for WMD, where the accuracy rises while comparing corpus with lengthy sequences. This can be attributed to establishing semantic relatedness of similar words in both documents instead of matching sub-sequences. S2SA-SNN being constituted from word-level representations, provides satisfactory accuracy for MSRPC having similar-length sequences for comparison. But for data-sets having unequal-length sequences like CNN/ Daily Mail and XSum, the accuracy drops considerably. In the case of TexIm V1, the performance improves due to informed contextualized representations. But, due to the dependency of the representations on the sequence length, the accuracy declines when comparing disparate length sequences. The performance improves further with TexIm FAST-C architecture similar to the proposed TexIm FAST, distinguished by the absence of the TSLFN block. When TexIm FAST representations are fed into the proposed STS model, overall 5.6% superior performance compared to TexIm FAST-C is obtained. Moreover, on the CNN/ Daily Mail and the XSum data-sets the improvement in accuracy is significantly high. This highlights the inability of existing approaches to deal with disparate length sequences and simultaneously the proficiency of the TexIm FAST representations as-well-as the proposed STS model to overcome this drawback.

### 5.4 Ablation Study

The effectiveness of the parameters used for the proposed TexIm FAST and the generated representations has been validated through a detailed ablation study.

#### 5.4.1 Image Dimensionality and Number of Channels

The dimensionality as-well-as the number of channels of the proposed TexIm FAST has been selected after analyzing the effectiveness in terms of information retained as-well-as efficiency in terms of memory footprint of the images. For this, various image dimensions and channel combinations have been studied as follows:

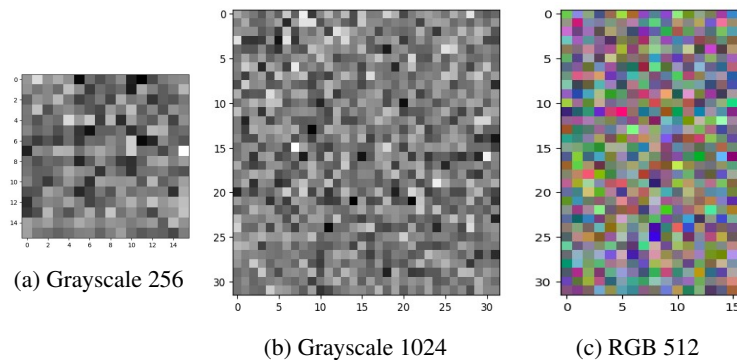


Figure 9: Sample representations generated by the model ablations upon the MSRPC Data-Set

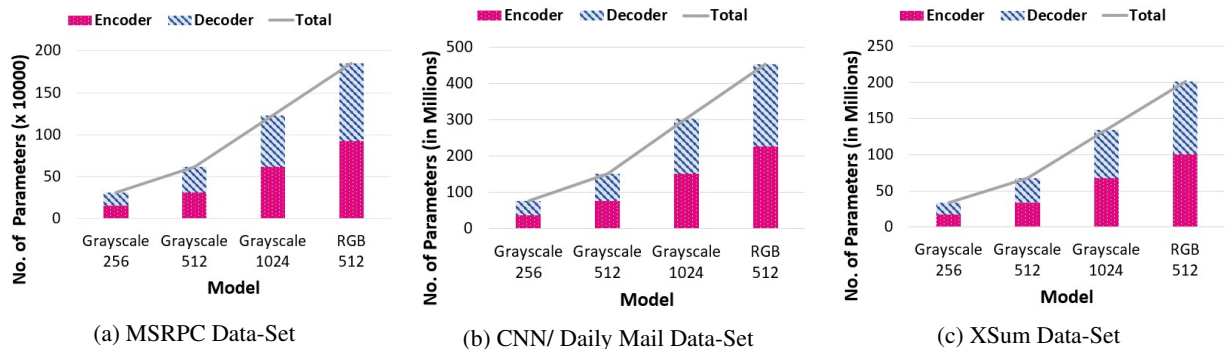


Figure 10: Comparison of the number of model parameters for ablations of TexIm FAST models upon various data-sets

- (i) **Grayscale 256:** A grayscale image having 256 pixels having length as 16 pixels and width as 16 pixels (specimen Figure 9a).

- (ii) **Grayscale 512 (Proposed Methodology)**: A grayscale image having  $32 \times 16$  pixels, i.e. 512 pixels. It is the selected dimensionality of the proposed TexIm FAST.
- (iii) **Grayscale 1024**: A grayscale image having  $32 \times 32$  pixels, i.e. 1024 pixels (specimen Figure 9b).
- (iv) **RGB 512**: RGB representations with three channels having  $32 \times 16 \times 3$  pixels, i.e. 1536 pixels (specimen Figure 9c).

Table 5: Analysis of Variation in Image Dimensionality and Number of Channels

Data-Set	Model	Accuracy	F1-Score
MSRPC	Grayscale 256	0.66	0.55
	Grayscale 512	<b>0.71</b>	0.63
	Grayscale 1024	0.68	0.62
	RGB 512	0.69	<b>0.64</b>
CNN/ Daily Mail	Grayscale 256	0.76	0.75
	Grayscale 512	0.81	0.80
	Grayscale 1024	0.82	0.82
	RGB 512	<b>0.86</b>	<b>0.86</b>
Xsum	Grayscale 256	0.77	0.75
	Grayscale 512	0.81	0.80
	Grayscale 1024	0.83	0.83
	RGB 512	<b>0.85</b>	<b>0.85</b>

Table 5 depicts the comparison of accuracy across the model ablations varying in the image dimensionality and number of channels while Figure 10 compares the number of parameters of the ablations. Here, it can be observed that with increasing dimensions the informativeness of the representations increases along with a decrease in memory efficiency. For a given image dimensionality, the shorter sequences are more informative compared to long sequences. Besides, the RGB representations provide the highest accuracy for the CNN/ Daily Mail and XSum data-sets comprising long sequences. For the MSRPC data-set with short sentences, while the F1-score is the highest, not much improvement can be noticed in terms of accuracy. This can be attributed to the fact that as the sequences are condensed into fixed-length representations, for shorter sequences more information can be packed while some information is lost in the case of long sequences. However, excessively larger images might not be effective beyond a certain extent due to information redundancy and rise in memory consumption. Furthermore, Figure 10 depicts that the number of model parameters rises with increasing resolution and number of channels. Therefore, the rise in performance comes at the cost of efficiency.

#### 5.4.2 Contribution of TexIm in STS

After analyzing the efficacy of the variations of TexIm FAST representations, the contribution of the TexIm encodings as a whole towards STS has been studied. For this, the performance of the proposed STS model is examined through the following ablations:

- (i) **Discrete STS**: This version comprises of the STS block isolated from the proposed TexIm FAST model. Here, the pre-processed input text is fed directly to the proposed STS model without any other transformations.
- (ii) **Tex FAST**: This is an ablation of the TexIm FAST wherein instead of generating the visual representations, the fixed-length encodings obtained from the proposed TexIm FAST model are directly fed into the STS model.

From the analysis of model ablations related to the inclusion of TexIm representations in Table 6, it can be inferred that Discrete STS falters in performance compared to TexIm FAST as the model input is devoid of the linguistic characteristics and contextual information imbibed in the TexIm FAST encodings. Additionally, the performance drops significantly for disparate-length sequences in the case of CNN/ Daily Mail and XSum data-sets due to absence of the fixed-length encodings like TexIm FAST. Besides, the Tex FAST slightly excels the proposed TexIm FAST. This

Table 6: Analysis of the Contribution of TexIm in STS

Data-Set	Method	Accuracy	F1-Score
MSRPC	Discrete STS	0.67	0.65
	Tex FAST	0.72	0.66
	TexIm FAST	0.71	0.63
CNN/ DailyMail	Discrete STS	0.59	0.57
	Tex FAST	0.81	0.81
	TexIm FAST	0.81	0.80
XSum	Discrete STS	0.57	0.54
	Tex FAST	0.81	0.80
	TexIm FAST	0.80	0.79

difference can be attributed to the loss of information due to the quantization performed in TexIm FAST. However, on estimating the accuracy versus efficiency trade-off in *Section 5.5*, this  $\approx 1\%$  drop in accuracy reduces the memory consumption by 75%.

Table 7: Comparison of Compression Capability

Representation	Conventional Approach	TexIm FAST	Compression Achieved
Plain text representation <sup>1</sup>	2123.57B	512B	75.89%
Word Embedding (Word2Vec) <sup>2</sup>	61440B	512B	99.92%
Word Embedding (BERT) <sup>3</sup>	1572864B	512B	99.97%
Sequence Embedding <sup>4</sup>	2048B	512B	75%
TexIm [26]	1536B	512B	66.67%

<sup>1</sup> Average memory required to store each sequence in the data-sets studied in this paper.

<sup>2</sup> Memory required to store a 512 length sequence using 300 dimensional Word2Vec word embeddings.

<sup>3</sup> Memory required to store a 512 length sequence using 768 dimensional BERT word embeddings.

<sup>4</sup> Memory required to store a 512 length sequence using sequence embedding having 512 dimensions.

## 5.5 Efficiency Evaluation

Comparing the efficiency in terms of model parameters as illustrated in Figure 10, it can be inferred that a rise in the image dimensionality and number of channels contribute to escalation in the model parameters leading to a decline in efficiency. For the MSRPC data-set, the number of parameters is the lowest while for the CNN/ Daily Mail the model parameters are the highest. Thus, the number of model parameters is proportional to the length of input sequences.

In terms of memory compression, the efficiency of the TexIm FAST representations compared to conventional text representation techniques has been analyzed in Table 7. Compared to plain text, the TexIm FAST representations provide compression for any sequences longer than 107 words. This is in consideration of the fact that in the English language, a word contains approximately 4.79 characters<sup>5</sup>. For word embedding techniques, the compression achieved is over 99%. For sequence embeddings, although the dimensionality of the vector remains the same, the compression is due to the application of unsigned int ('uint8') notation in TexIm FAST in place of 32-bit float ('float32') notation adopted in conventional embeddings. Moreover, over 66% compression is achieved compared to TexIm [26] due to single-channel grayscale representations in place of three-channel RGB representations. Overall, it can be observed that the proposed TexIm FAST achieves above 75% compression in terms of memory footprint compared to the conventional representation techniques.

<sup>5</sup><http://www.norvig.com/mayzner.html>



## 5.6 Applications of TexIm FAST

Apart from STS, the TexIm FAST representations are potent enough to be applied to a wide variety of downstream tasks. In spite of being indecipherable to the human eye, the representations can serve as input to models for further analysis enabling oblivious inference. This makes it appropriate for applications involving sensitive data such as patient records, customer repository and defence related data. In such applications, the TexIm FAST representations can be stored in the servers and used for further processing instead of performing the operations on the original data to ensure privacy. Moreover, the TexIm FAST representations are irreversible. Thus, even if some malicious agent obtains these representations, the actual text cannot be recovered from it. Furthermore, TexIm FAST significantly reduces the input memory requirements for downstream tasks making it deployable to devices with limited computational power.

## 6 Conclusion

This paper augments the body of knowledge through a self-supervised architecture titled TexIm FAST for generating fixed-length pictorial representations from text. The representations allow oblivious inference by retaining the linguistic intricacies of the original text along with a reduction in the memory footprint by over 75%. Furthermore, a novel transformer encoder architecture has been formulated for STS. The efficacy of the proposed TexIm FAST has been analyzed through an extensive set of experiments. The results demonstrate that the proposed methodologies excel in the task of STS, and deliver noteworthy performance when dealing with disparate length sequences. However, encoding variable-length sequences to fixed-length representations implies that for smaller sequences the amount of information retained is higher and reduces as the sequence length increases. Therefore, an adaptive approach can be devised to determine the image resolution based on the sequence length. In the future, the potential of TexIm FAST can be examined on a wide range of NLP tasks as-well-as image processing models. This paper ushers a new avenue of text-to-image representation, with ample scope for formulating more effective as-well-as efficient techniques for cross-modal analysis of text.

## Acknowledgments

None. The author(s) received no financial or any other kinds of support for the research, authorship, and/or publication of this article.

## References

- [1] Lu, Nijia, Guohua Wu, Zhen Zhang, Yitao Zheng, Yizhi Ren, and Kim-Kwang Raymond Choo. "Cyberbullying detection in social media text based on character-level convolutional neural network with shortcuts." *Concurrency and Computation: Practice and Experience* 32, no. 23 (2020): e5627.
- [2] Hu, Linmei, Zeyi Liu, Ziwang Zhao, Lei Hou, Liqiang Nie, and Juanzi Li. "A survey of knowledge enhanced pre-trained language models." *IEEE Transactions on Knowledge and Data Engineering* (2023).
- [3] Suman, Chanchal, Saichethan Miriyala Reddy, Sriparna Saha, and Pushpak Bhattacharyya. "Why pay more? A simple and efficient named entity recognition system for tweets." *Expert Systems with Applications* 167 (2021): 114101.
- [4] Omuya, Erick Odhiambo, George Okeyo, and Michael Kimwele. "Sentiment analysis on social media tweets using dimensionality reduction and natural language processing." *Engineering Reports* 5, no. 3 (2023): e12579.
- [5] Zakraoui, Jezia, Moutaz Saleh, and Al Ja'am. "Text-to-picture tools, systems, and approaches: a survey." *Multimedia Tools and Applications* 78, no. 16 (2019): 22833-22859.
- [6] Nataraj, Lakshmanan, Sreejith Karthikeyan, Gregoire Jacob, and Bangalore S. Manjunath. "Malware images: visualization and automatic classification." In *Proceedings of the 8th international symposium on visualization for cyber security*, pp. 1-7. 2011.
- [7] He, K., & Kim, D.-S. (2019). Malware Detection with Malware Images using Deep Learning Techniques. 2019 18th IEEE International Conference On Trust, Security And Privacy In Computing And Communications/13th IEEE International Conference On Big Data Science And Engineering (TrustCom/BigDataSE). doi:10.1109/TrustCom/BigDataSE.2019.00022
- [8] Petrie, Stephen M., and T'Mir D. Julius. "Representing text as abstract images enables image classifiers to also simultaneously classify text." *arXiv preprint arXiv:1908.07846* (2019).

- [9] Chandrasekaran, Dhivya, and Vijay Mago. "Evolution of semantic similarity—a survey." *ACM Computing Surveys (CSUR)* 54, no. 2 (2021): 1-37.
- [10] El-Kassas, Wafaa S., Cherif R. Salama, Ahmed A. Rafea, and Hoda K. Mohamed. "Automatic text summarization: A comprehensive survey." *Expert systems with applications* 165 (2021): 113679.
- [11] Foltýnek, Tomáš, Norman Meuschke, and Bela Gipp. "Academic plagiarism detection: a systematic literature review." *ACM Computing Surveys (CSUR)* 52, no. 6 (2019): 1-42.
- [12] Soares, Marco Antonio Calijorne, and Fernando Silva Parreiras. "A literature review on question answering techniques, paradigms and systems." *Journal of King Saud University-Computer and Information Sciences* 32, no. 6 (2020): 635-646.
- [13] Dabre, Raj, Chenhui Chu, and Anoop Kunchukuttan. "A survey of multilingual neural machine translation." *ACM Computing Surveys (CSUR)* 53, no. 5 (2020): 1-38.
- [14] Lin, Chin-Yew. "Rouge: A package for automatic evaluation of summaries." In *Text summarization branches out*, pp. 74-81. 2004.
- [15] Papineni, Kishore, Salim Roukos, Todd Ward, and Wei-Jing Zhu. "Bleu: a method for automatic evaluation of machine translation." In *Proceedings of the 40th annual meeting of the Association for Computational Linguistics*, pp. 311-318. 2002.
- [16] Rodrigues, Joao, Chakaveh Saedi, António Branco, and Joao Silva. "Semantic Equivalence Detection: Are Interrogatives Harder than Declaratives?." In *Proceedings of the Eleventh International Conference on Language Resources and Evaluation (LREC 2018)*. 2018.
- [17] Sánchez, David, and Montserrat Batet. "A semantic similarity method based on information content exploiting multiple ontologies." *Expert Systems with Applications* 40, no. 4 (2013): 1393-1399.
- [18] Jiang, Yuncheng, Xiaopei Zhang, Yong Tang, and Ruihua Nie. "Feature-based approaches to semantic similarity assessment of concepts using Wikipedia." *Information Processing & Management* 51, no. 3 (2015): 215-234.
- [19] Cilibrasi, Rudi L., and Paul MB Vitanyi. "The google similarity distance." *IEEE Transactions on knowledge and data engineering* 19, no. 3 (2007): 370-383.
- [20] Kusner, Matt, Yu Sun, Nicholas Kolkin, and Kilian Weinberger. "From word embeddings to document distances." In *International conference on machine learning*, pp. 957-966. PMLR, 2015.
- [21] Wang, Zhiguo, Haitao Mi, and Abraham Ittycheriah. "Sentence Similarity Learning by Lexical Decomposition and Composition." In *Proceedings of COLING 2016, the 26th International Conference on Computational Linguistics: Technical Papers*, pp. 1340-1349. 2016.
- [22] He, Hua, and Jimmy Lin. "Pairwise word interaction modeling with deep neural networks for semantic similarity measurement." In *Proceedings of the 2016 conference of the north American chapter of the Association for Computational Linguistics: human language technologies*, pp. 937-948. 2016.
- [23] Tien, Nguyen Huy, Nguyen Minh Le, Yamasaki Tomohiro, and Izuha Tatsuya. "Sentence modeling via multiple word embeddings and multi-level comparison for semantic textual similarity." *Information Processing & Management* 56, no. 6 (2019): 102090.
- [24] Lopez-Gazpio, Inigo, Montse Maritxalar, Mirella Lapata, and Eneko Agirre. "Word n-gram attention models for sentence similarity and inference." *Expert Systems with Applications* 132 (2019): 1-11.
- [25] Li, Zhengguang, Heng Chen, and Huayue Chen. "Biomedical text similarity evaluation using attention mechanism and Siamese neural network." *IEEE Access* 9 (2021): 105002-105011.
- [26] Ansar, Wazib, Saptarsi Goswami, Amlan Chakrabarti, and Basabi Chakraborty. "TexIm: A Novel Text-to-Image Encoding Technique Using BERT." In *Computer Vision and Machine Intelligence: Proceedings of CVMI 2022*, pp. 123-139. Singapore: Springer Nature Singapore, 2023.
- [27] Subramanian, Sandeep, Sai Rajeswar Mudumba, Alessandro Sordani, Adam Trischler, Aaron C. Courville, and Chris Pal. "Towards text generation with adversarially learned neural outlines." *Advances in Neural Information Processing Systems* 31 (2018).
- [28] Zhang, Xinqiao, Mohammad Samragh, Siam Hussain, Ke Huang, and Farinaz Koushanfar. "Scalable Binary Neural Network applications in Oblivious Inference." *ACM Transactions on Embedded Computing Systems* (2023).
- [29] Yang, Erkun, Cheng Deng, Chao Li, Wei Liu, Jie Li, and Dacheng Tao. "Shared predictive cross-modal deep quantization." *IEEE transactions on neural networks and learning systems* 29, no. 11 (2018): 5292-5303.

- [30] Xu, Xing, Tan Wang, Yang Yang, Lin Zuo, Fumin Shen, and Heng Tao Shen. "Cross-modal attention with semantic consistence for image–text matching." *IEEE transactions on neural networks and learning systems* 31, no. 12 (2020): 5412-5425.
- [31] Jin, Lu, Zechao Li, and Jinhui Tang. "Deep semantic multimodal hashing network for scalable image-text and video-text retrievals." *IEEE Transactions on Neural Networks and Learning Systems* (2020).
- [32] Das, Anindya Sundar, and Sriparna Saha. "Self-supervised Image-to-Text and Text-to-Image Synthesis." In *Neural Information Processing: 28th International Conference, ICONIP 2021, Sanur, Bali, Indonesia, December 8–12, 2021, Proceedings, Part IV 28*, pp. 415-426. Springer International Publishing, 2021.
- [33] Ramesh, Aditya, Mikhail Pavlov, Gabriel Goh, Scott Gray, Chelsea Voss, Alec Radford, Mark Chen, and Ilya Sutskever. "Zero-shot text-to-image generation." In *International Conference on Machine Learning*, pp. 8821-8831. PMLR, 2021.
- [34] Saharia, Chitwan, William Chan, Saurabh Saxena, Lala Li, Jay Whang, Emily L. Denton, Kamyar Ghasemipour et al. "Photorealistic text-to-image diffusion models with deep language understanding." *Advances in Neural Information Processing Systems* 35 (2022): 36479-36494.
- [35] Gu, Shuyang, Dong Chen, Jianmin Bao, Fang Wen, Bo Zhang, Dongdong Chen, Lu Yuan, and Baining Guo. "Vector quantized diffusion model for text-to-image synthesis." In *Proceedings of the IEEE/CVF Conference on Computer Vision and Pattern Recognition*, pp. 10696-10706. 2022.
- [36] Tan, Hongchen, Xiuping Liu, Baocai Yin, and Xin Li. "DR-GAN: Distribution regularization for text-to-image generation." *IEEE Transactions on Neural Networks and Learning Systems* (2022).
- [37] Wu, Yonghui, Mike Schuster, Zhifeng Chen, Quoc V. Le, Mohammad Norouzi, Wolfgang Macherey, Maxim Krikun et al. "Google’s neural machine translation system: Bridging the gap between human and machine translation." *arXiv preprint arXiv:1609.08144* (2016).
- [38] Zhen, Liangli, Peng Hu, Xi Peng, Rick Siow Mong Goh, and Joey Tianyi Zhou. "Deep multimodal transfer learning for cross-modal retrieval." *IEEE Transactions on Neural Networks and Learning Systems* 33, no. 2 (2020): 798-810.
- [39] Vaswani, Ashish, Noam Shazeer, Niki Parmar, Jakob Uszkoreit, Llion Jones, Aidan N. Gomez, Łukasz Kaiser, and Illia Polosukhin. "Attention is all you need." *Advances in neural information processing systems* 30 (2017).
- [40] Ansar, Wazib, Saptarsi Goswami, Amlan Chakrabarti, and Basabi Chakraborty. "A novel selective learning based transformer encoder architecture with enhanced word representation." *Applied Intelligence* (2022): 1-20.
- [41] Goodfellow, Ian, Yoshua Bengio, and Aaron Courville. *Deep learning*. MIT press, 2016.
- [42] Liu, Danyang, and Gongshen Liu. "A transformer-based variational autoencoder for sentence generation." In *2019 International Joint Conference on Neural Networks (IJCNN)*, pp. 1-7. IEEE, 2019.
- [43] Dolan, Bill, and Chris Brockett. "Automatically constructing a corpus of sentential paraphrases." In *Third International Workshop on Paraphrasing (IWP2005)*. 2005.
- [44] Nallapati, Ramesh, Bowen Zhou, Cicero dos Santos, Caglar Gulcehre, and Bing Xiang. "Abstractive Text Summarization using Sequence-to-sequence RNNs and Beyond." In *Proceedings of The 20th SIGNLL Conference on Computational Natural Language Learning*, p. 280. Association for Computational Linguistics, 2016.
- [45] Narayan, Shashi, Shay Cohen, and Maria Lapata. "Don’t Give Me the Details, Just the Summary! Topic-Aware Convolutional Neural Networks for Extreme Summarization." In *2018 Conference on Empirical Methods in Natural Language Processing*, pp. 1797-1807. Association for Computational Linguistics, 2018.